

Growth, spectroscopy and laser operation of Yb:KGd(PO₃)₄ single crystals

I. Parreu, M. C. Pujol, M. Aguiló, and F. Díaz

*Física i Cristal·lografia de Materials (FiCMA), Universitat Rovira i Virgili.
c/ Marcel·lí Domingo, s/n. E-43007 Tarragona, Spain.
f.diaz@urv.cat*

X. Mateos and V. Petrov

Max-Born-Institute for Nonlinear Optics and Ultrafast Spectroscopy, 2A Max-Born Str., D-12489 Berlin, Germany.

Abstract: Macrodefect-free single crystals of Yb-doped KGd(PO₃)₄, a noncentrosymmetric laser host which possesses second-order nonlinear susceptibility, were grown using the top seeded solution growth slow-cooling (TSSG-SC) technique, reaching a maximum ytterbium concentration in the crystal of $\approx 3.2 \times 10^{20}$ at/cm³. In order to evaluate the potential for self-frequency doubling, the dispersion of the refractive indices of KGd(PO₃)₄ was studied and Sellmeier equations were constructed which are valid in the visible and near-infrared. The Stark splitting of the two electronic states of ytterbium was determined from absorption and emission measurements at room and low temperatures, and this allowed to compute the emission cross sections at room temperature. The fluorescence decay time is quite long, 1.22 ± 0.01 ms. Laser generation in the 1 μ m range is demonstrated with this new Yb host for the first time. Although the maximum output power achieved, of the order of 100 mW, was limited by the available crystal size and doping level, the more than 55% slope efficiency obtained with this first sample is rather promising for the future.

© 2007 Optical Society of America

OCIS codes: (140.3580) Lasers, solid-state; (140.5680) Rare earth and transition metal solid-state lasers; (160.5690) Rare earth doped materials; (190.4400) Nonlinear optics, materials

References and links

1. A. Brenier, "The self-doubling and summing lasers: overview and modeling," *J. Lumin.* **91**, 121 (2000).
2. A. Aron, G. Aka, B. Viana, A. Kahn-Harari, D. Vivien, F. Druon, F. Balembos, P. Georges, A. Brun, N. Lenain, and M. Jaquet, "Spectroscopic properties and laser performances of Yb:YCOB and potential of the Yb:LaCOB material," *Opt. Mater.* **16**, 181 (2001).
3. H. Zhang, X. Meng, P. Wang, L. Zhu, X. S. Liu, X. M. Liu, Y. Yang, R. Wang, J. Dawes, J. A. Piper, S. Zhang, and L. Sun, "Growth of Yb-doped Ca₄GdO(BO₃)₃ crystals and their spectra and laser properties," *J. Cryst. Growth* **222**, 209 (2001).
4. P. Dekker, P. A. Burns, J. M. Dawes, and J. A. Piper, "Widely tunable yellow-green lasers based on the self-frequency-doubling material Yb:YAB," *J. Opt. Soc. Am. B* **20**, 706 (2003).
5. Z. Zhu, J. Li, B. Alain, G. Jia, Z. You, X. Lu, B. Wu and C. Tu, "Growth, spectroscopic and laser properties of Yb³⁺-doped GdAl₃(BO₃)₄ crystal: a candidate for infrared laser crystal," *Appl. Phys. B* **86**, 71 (2007).
6. L.E. Bausá, M. O. Ramírez, and E. Montoya, "Optical performance of Yb³⁺ in LiNbO₃ laser crystal," *Phys. Status Solidi (a)* **201**, 289 (2004).
7. I. Parreu, J. J. Carvajal, X. Solans, F. Díaz, and M. Aguiló, "Crystal structure and optical characterization of pure and Nd-substituted type III KGd(PO₃)₄," *Chem. Mater.* **18**, 221 (2006).
8. I. Parreu, R. Solé, Jna. Gavalda, J. Massons, F. Díaz, and M. Aguiló, "Crystal growth, structural characterization, and linear thermal evolution of KGd(PO₃)₄," *Chem. Mater.* **17**, 822 (2005).
9. I. Parreu, R. Solé, J. Massons, F. Díaz, and M. Aguiló, "Crystal Growth and Characterization of type III ytterbium-doped KGd(PO₃)₄: a new non-linear laser host" (submitted to *Chem. Mater.*).

10. H. Ettis, H. Naïli, and T. Mhiri, "Synthesis and crystal structure of a new potassium-gadolinium cyclotetraphosphate, $\text{KGdP}_4\text{O}_{12}$," *Cryst. Growth and Design*, **3**, 599 (2003).
11. R. Solé, V. Nikolov, A. Vilalta, J. J. Carvajal, J. Massons, Jna. Gavalda, M. Aguiló, and F. Díaz, "Growth of KTiOPO_4 films on $\text{KTi}_{1-x}\text{Ge}_x\text{OPO}_4$ substrates by liquid-phase epitaxy," *J. Mater. Res.* **17**, 563 (2002).
12. M. Born and E. Wolf, in *Principles of Optics: Electromagnetic Theory of Propagation, Interference and Diffraction of Light*, 6th.ed. (Pergamon, Oxford 1993).
13. P. Tzankov and V. Petrov, "Effective second-order nonlinearity in acentric optical crystals with low symmetry," *Appl. Opt.* **44**, 6971 (2005).
14. F. D. Patel, E. C. Honea, J. Speth, S.A. Payne, R. Hutcheson, and R. Equall, "Laser demonstration of $\text{Yb}_3\text{Al}_5\text{O}_{12}$ (YbAG) and materials properties of highly doped Yb:YAG," *IEEE J. Quantum Electron.* **37**, 135 (2001).

1. Introduction

Solid-state laser sources in the visible play an important role in laser technology because they are potentially interesting for numerous applications like high-density optical data storage or laser displays. Bifunctional crystals, in which the laser effect and a nonlinear optical process, e.g. frequency doubling, occur simultaneously, are very promising for such compact laser designs because diode-pumped solid-state lasers operate mainly in the infrared. So far the noncentrosymmetric hosts used for this purpose were doped mainly with neodymium [1]. More recently highly efficient laser operation in several crystals exhibiting second order nonlinearity, doped with ytterbium, was also reported. These include $\text{YCa}_4\text{O}(\text{BO}_3)_3$ (YCOB) [2], $\text{GdCa}_4\text{O}(\text{BO}_3)_3$ (GdCOB) [3], $\text{YAl}_3(\text{BO}_3)_4$ (YAB) [4], $\text{GdAl}_3(\text{BO}_3)_4$ (GAB) [5], and LiNbO_3 (LNB) [6]. The ytterbium ion is an interesting alternative to neodymium in the same wavelength range near $1\ \mu\text{m}$ while the second harmonic is also in the green region. This is due to several important advantages. The ytterbium ion possesses higher energy-storage capability because the radiative lifetime of the upper laser manifold is substantially longer. Its simple two-manifold electronic structure excludes a number of competitive processes such as excited-state absorption, upconversion, and cross relaxation which can depopulate the upper laser level and hence reduce the laser efficiency. The small Stokes shift between absorption and emission, i.e. the small quantum defect, reduces the thermal load and facilitates efficient operation at high powers. The development of new Yb-doped laser materials is motivated by the significant advance in diode laser pumps; such lasers can be pumped by the more robust InGaAs diodes delivering high powers in the $0.9\text{--}1\ \mu\text{m}$ range. Finally, ytterbium has no bands in the green region, so the inevitable reabsorption losses of neodymium in the wavelength range of the second harmonic can be avoided.

In this paper, we propose a new candidate for self-frequency doubling laser material, Yb-doped $\text{KGd}(\text{PO}_3)_4$ (KGP). The present work is devoted primarily to spectroscopic investigations, i.e. polarized absorption and fluorescence measurements at room and low temperatures, and lifetime measurements for the upper laser level at room temperature. We report also, for the first time to our knowledge, room temperature laser operation near $1\ \mu\text{m}$ of $\text{KYb}_{0.024}\text{Gd}_{0.976}(\text{PO}_3)_4$, in the continuous-wave regime. In addition, we verify that this crystal is phase-matchable for second harmonic generation in the wavelength range covered by the ytterbium ion.

The host KGP is a monoclinic acentric crystal with the space group $P2_1$ [7]. KGP exhibits a broad transmission window extending from about $180\ \text{nm}$ to $4\ \mu\text{m}$ which covers both the fundamental and the second harmonic range. The rather large band-gap, on one hand, should lead to high damage resistivity, on the other hand it allows in principle the use of this host also in the UV range (either as a nonlinear crystal or as a host for cerium). Another advantage of KGP is its almost isotropic thermal expansion [7] which is important for the crystal growth, processing of laser elements, and during laser operation. The high hardness of KGP, close to that of quartz in the Moh's scale, facilitates sample preparation and allows polishing the surfaces with good optical quality. KGP is also chemically stable against moisture as well as against weakly acidic and basic media.

We were able to grow inclusion and macrodefect-free single crystals of Yb:KGP by partial replacement of gadolinium by ytterbium, using the top seeded solution growth-slow cooling (TSSG-SC) technique. Up to now, it was possible to grow single crystals of KGP with ytterbium concentration in the solution as high as 15 at % [9]. This corresponds to ≈ 7.5 at % in the bulk crystal since the actual ytterbium concentration in the crystal was found to be reduced to about half of that in the solution (Table 1). The composition of the Yb:KGP crystals was studied by electron probe microanalysis (EPMA) using a Cameca SX 50 equipment operating at an accelerating voltage of 20 kV and electron current of 100 nA.

Table 1. EPMA results for Yb:KGP. K_{Ln} denotes the distribution coefficient of the lanthanide ions in the crystal

Yb at % in solution	K_{Yb}	K_{Gd}	Yb concentration (cm^{-3})	chemical formula
1	0.50	1.01	2.081×10^{19}	$\text{KYb}_{0.005}\text{Gd}_{0.995}(\text{PO}_3)_4$
3	0.53	1.01	6.656×10^{19}	$\text{KYb}_{0.016}\text{Gd}_{0.984}(\text{PO}_3)_4$
5	0.48	1.03	1.007×10^{20}	$\text{KYb}_{0.024}\text{Gd}_{0.976}(\text{PO}_3)_4$
10	0.40	1.07	1.653×10^{20}	$\text{KYb}_{0.040}\text{Gd}_{0.960}(\text{PO}_3)_4$
15	0.51	1.02	3.203×10^{20}	$\text{KYb}_{0.077}\text{Gd}_{0.923}(\text{PO}_3)_4$

Although the dopant acceptance seemed not to be limited by the ionic radius of ytterbium ion we found it difficult to incorporate high concentrations of ytterbium in the KGP structure. In fact, the problem was related to the crystallization of the monoclinic but centrosymmetric phase $C2/c$ [10] instead of the desired structure $P2_1$ [7]. Further investigations on the crystallization region of the $P2_1$ -phase of Yb:KGP indicate that this phase could crystallize from solutions with an ytterbium concentration as high as 50 at %. Thus, assuming that the ytterbium concentration in the crystal would be reduced again by about a half, it can be expected that doping levels as high as 25-30 at %, i.e. $\approx 1 \times 10^{21} \text{ cm}^{-3}$, might be reached in single crystals grown by the TSSG-SC method [9]. All results on Yb:KGP reported in this paper are based on a single growth of the composition $\text{KYb}_{0.024}\text{Gd}_{0.976}(\text{PO}_3)_4$ corresponding to an ytterbium concentration of $1.007 \times 10^{20} \text{ cm}^{-3}$. To avoid impurities in the grown crystal, it was obtained from its self-flux and the optimized solution composition was $\text{Yb}_2\text{O}_3:\text{Gd}_2\text{O}_3:\text{K}_2\text{O}:\text{P}_2\text{O}_5=0.3:5.7:34:60 \text{ mol } \%$. Because of the high viscosity of the solution, around 2 Dp, the seed holder was equipped with a platinum turbine rotating at the rather high velocity of 75 rpm. The axial temperature gradient was about 1.2 K/mm. The saturation temperature amounted to 958 K. The temperature of the solution was decreased to 12 K below the saturation temperature at a rate of 0.05 K/h. An a^* -oriented parallelepipedic seed of undoped KGP was used to grow the crystal.

2. Optical Characterization of the KGP host

In a previous publication we characterized the undoped KGP in terms of transmission window and orientation of the optical ellipsoid [8]. The UV transmission edge of Yb-doped KGP is slightly shifted to the visible due to the presence of ytterbium and the cut-off wavelength is 200 nm [9]. The orientation of the three principal optical axes of KGP, denoted as N_p , N_m , and N_g , according to the refractive indices $n_p < n_m < n_g$, was determined with respect to the crystallographic frame (a , b , c) at a wavelength of 632.8 nm. For a monoclinic crystal, one of the principal optical axes coincides with the b crystallographic axis; in the case of KGP this is N_p . N_g was found to lie at 37.3° clockwise from the c crystallographic axis with the positive direction of the b axis towards the observer.

In order to establish if self-frequency doubling is possible in Yb:KGP we examined as a first step the dispersion of the three refractive indices of undoped KGP (Fig. 1). The refractive indices were measured between 0.45 and $1.2 \mu\text{m}$ with two semiprisms [11], oriented for measurement of n_p - n_m and n_p - n_g , respectively, using the minimum deviation method. The accuracy of the measurements was 10^{-4} .

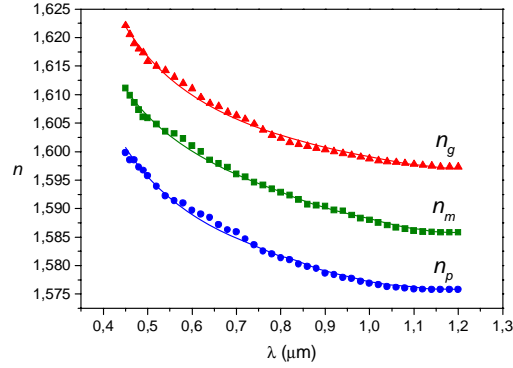


Fig. 1. Dispersion of the principal refractive indices of KGP at room temperature.

As can be seen from Fig. 1 the three refractive indices are nearly equidistant. KGP is an optically negative biaxial crystal since the $2V_g$ angle between the two optic axes [12], lying in the N_p - N_g plane, is 94.2° at 632.8 nm. The data points in Fig. 1 were fitted using one UV pole and an IR correction term with the Sellmeier equation,

$$n^2 = A + B/[1-(C/\lambda)^2] - D\lambda^2$$

Table 2 summarizes the Sellmeier coefficients obtained for KGP at room temperature.

Principal refractive index	A	B	C (μm)	D (μm ⁻²)
n_p	1.7404	0.7479	0.1374	0.0138
n_m	1.7624	0.7667	0.1304	0.0193
n_g	1.7728	0.7782	0.1391	0.0091

Estimations based on these Sellmeier equations indicate that KGP is phase-matchable for type-I second harmonic generation near 1 μm both in the N_p - N_m (oo-e type interaction) and in the N_m - N_g (ee-o type interaction) principal planes. It should be outlined that biaxial crystals have in general greater potential for self-frequency doubling because they offer greater variety of phase-matching configurations. Considering for instance the preferable type-I interaction, uniaxial crystals allow only one phase-matching configuration (oo-e or ee-o depending on whether they are negative or positive). As can be seen in the case of KGP, both oo-e and ee-o phase-matching are possible and their effective nonlinearity is nonvanishing for point group 2 [13]. Thus one has greater freedom to select the polarization of the fundamental in such a way that the gain is also maximized.

3. Spectroscopic Characterization of Yb:KGP

All further results reported here were based on a single Yb-doped KGP sample which was cut and polished as a cube, accurately oriented along the N_p , N_m , and N_g principal optical axes, with dimensions of 2.34, 2.68, and 2.47 mm along these axes, respectively.

The polarized optical absorption of $\text{KYb}_{0.024}\text{Gd}_{0.976}(\text{PO}_3)_4$ in the temperature range from 6 to 300 K was measured using a Cary Varian 500 spectrophotometer equipped with a Leybold RDK-6-320 closed-cycle helium cryostat. The absorption band associated with the ytterbium transition $^2F_{7/2} \rightarrow ^2F_{5/2}$ in KGP extends from 9750 to 10800 cm^{-1} (1025-925 nm) at room temperature (Fig. 2). It is characterized by three main peaks centered at 10230, 10305 and 10586 cm^{-1} . As ytterbium has an odd number of electrons in the 4f shell, polarization dependent selection rules are not expected but the intensity of the individual peaks may still vary. The anisotropy observed in the absorption spectra of Yb:KGP is rather low and the

absorption cross-section is maximized for $E//N_m$. Its maximum value at 977 nm (zero line transition), calculated with the exact Yb^{3+} concentration of $1.007 \times 10^{20} \text{ cm}^{-3}$, amounts to $1.17 \times 10^{-20} \text{ cm}^2$. For $E//N_g$ and N_p , the corresponding maximum absorption cross sections at the same wavelength amount to 0.72×10^{-20} and $0.80 \times 10^{-20} \text{ cm}^2$. Fig. 2 shows the evolution of the absorption coefficient for $E//N_m$ with the temperature from 6 to 300 K. From the lowest temperature spectra we determined the energies of the three Stark sublevels of the excited state multiplet $^2F_{5/2}$. These energies are indicated in the inset of Fig. 2 where the levels are designated as $^2F_{5/2}(0')$, $(1')$, and $(2')$. When the temperature is increased, an additional peak emerges at 10140 cm^{-1} which is probably related to the thermal population of the $^2F_{7/2}(1)$ sublevel with transition to $^2F_{5/2}(0')$ but it is smoothed at room temperature.

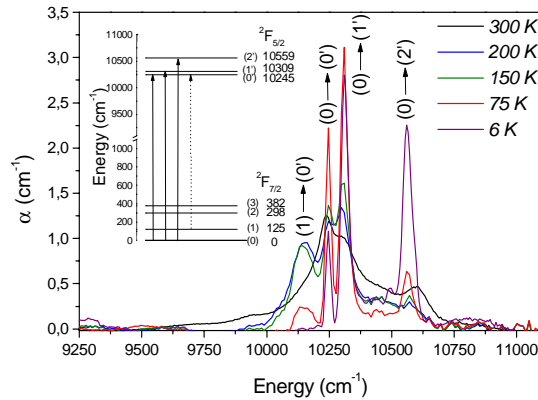


Fig. 2. Temperature evolution of the optical absorption of $\text{KYb}_{0.024}\text{Gd}_{0.976}(\text{PO}_3)_4$ for $E//N_m$. Inset: schematic diagram of the Stark sublevels and absorption transitions.

The fluorescence spectra were recorded at both 300 and 10 K in a 90° geometry. Excitation was provided by a 200 mW InGaAs diode laser emitting at 940 nm which was modulated at 1 kHz. The fluorescence was dispersed by a 0.46 m double monochromator (Jobin Yvon - Spex HR 460). The detector was a cooled Hamamatsu NIR R5509-72 photomultiplier connected to a lock-in amplifier (EG&G, 7265 DSP). A closed-cycle helium cryostat (Oxford CCC1104) was used to cool the sample for the low temperature measurements.

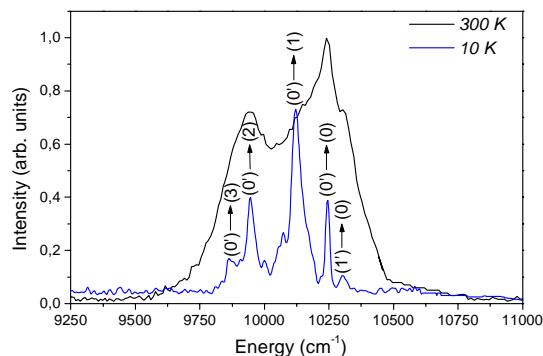


Fig. 3. Emission spectra at 300 K (solid line) and 10 K (dash-dotted line) for $E//N_m$

From the low-temperature polarized fluorescence spectra (Fig. 3) we determined the four sublevels of the ground state $^2F_{7/2}$. Four main lines were found at 10245, 10120, 9947 and 9863 cm^{-1} accompanied by phonon added peaks. These correspond to the transitions

$^2F_{5/2}(0') \rightarrow ^2F_{7/2}(0)$, $^2F_{5/2}(0') \rightarrow ^2F_{7/2}(1)$, $^2F_{5/2}(0') \rightarrow ^2F_{7/2}(2)$, and $^2F_{5/2}(0') \rightarrow ^2F_{7/2}(3)$, respectively. A dim peak corresponding to the transition from the thermally populated $^2F_{5/2}(1')$ sublevel to $^2F_{7/2}(0)$ is also seen at 10305 cm^{-1} . The reduced intensity of the emission associated with the $^2F_{5/2}(0') \rightarrow ^2F_{7/2}(0)$ transition is a consequence of the reabsorption at this wavelength. The Stark sublevels of the ground state manifold $^2F_{7/2}$, derived from the 10 K spectrum, are at 0, 125, 298, and 382 cm^{-1} .

The reciprocity method [14] was used to compute the emission cross sections from the absorption cross sections at room temperature and the determined level positions. Fig. 4 shows the calculated emission cross-sections σ_e together with the corresponding absorption cross sections σ_a for the three orthogonal polarizations.

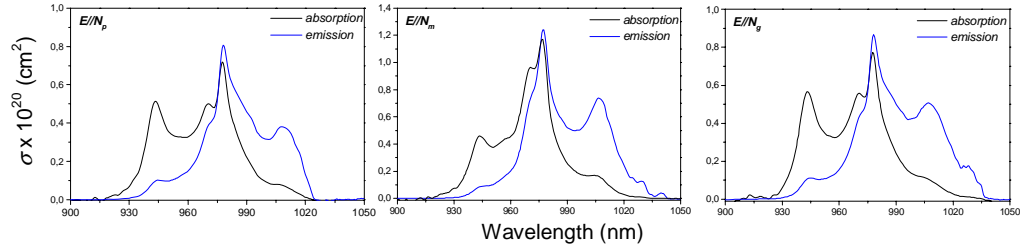


Fig. 4. Measured absorption and calculated emission cross-sections of Yb:KGP at room temperature for the three orthogonal polarizations.

By averaging the calculated $\sigma_e(\nu)$ by the reciprocity method over the three polarizations, a radiative lifetime of $\tau_{rad}=1.57\text{ ms}$ was obtained at room temperature using the F  chtbauer-Ladenburg equation [14]. The fluorescence decay time was measured by the pinhole method which avoids radiation trapping (Fig. 5). The extrapolated for zero diameter result, at room temperature, was $1.22 (\pm 0.01)\text{ ms}$ but the deviation from this value for all the pinhole diameters used, between 0.6 and 2.1 mm, was only $\pm 1\%$. Thus, reabsorption was negligible in $\text{KYb}_{0.024}\text{Gd}_{0.976}(\text{PO}_3)_4$ probably because of the low ion doping level in the crystal. This leads to an intrinsic quantum efficiency of 78%. Comparing the spectroscopic results with the available data on other acentric Yb-hosts such as Yb:YCOB [2], Yb:GdCOB [3], and Yb:YAB [4], it can be concluded that one feature which distinguishes Yb:KGP is the relatively short oscillation wavelength that can be expected. From Fig. 4, lasing can be expected on the $^2F_{5/2}(0') \rightarrow ^2F_{7/2}(2)$ transition, at wavelengths near 1010 nm. This was confirmed in the following laser experiments.

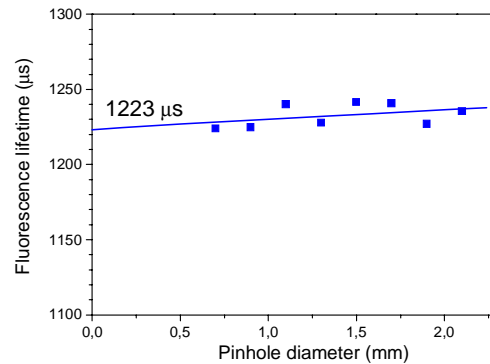


Fig. 5. Dependence of the fluorescence lifetime of $\text{KYb}_{0.024}\text{Gd}_{0.976}(\text{PO}_3)_4$ on the pinhole diameter.

4. Laser operation of Yb:KGP

A standard astigmatically compensated Z-shaped cavity was used as a laser setup. The pump source was a home-made Ti:sapphire laser (960-1025 nm, FWHM<1 nm, max. 3 W). The estimated pump waist in the focus of the $f=6.28$ cm anti-reflection coated lens was $\approx 30 \mu\text{m}$. The resonator (depicted in Fig. 6) contained two folding mirrors (M1 and M2), and two plane reflectors (rear mirror M3 and output coupler M4). M2 was highly transmitting at the pump wavelength (977.1 nm). The pumping was in a single-pass. The transmission of the output coupler T_{oc} ranged from 1 to 5%.

The uncoated Yb:KGP sample was attached to a Cu-holder without active cooling and positioned under Brewster angle between the two folding mirrors. We tried to pump this sample with all possible polarizations. Continuous-wave laser operation was obtained for the first time in this monoclinic material at room temperature for pumping with $E//N_m$ (propagation along N_g) and with $E//N_p$ (propagation again along N_g). The laser always had the same polarization as the pump due to the Brewster orientation. No generation was possible for pumping with $E//N_g$ although we tried this for propagation both along N_m and along N_p .

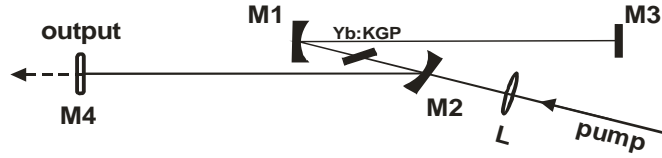


Fig. 6. Laser set-up: Total cavity length, 129 cm; M1 and M2 are curved mirrors with radius of curvature ~ 100 mm, and M3 (rear reflector) and M4 (output coupler with transmission $T_{oc}=1, 3$, or 5 %) are plane mirrors.

The input-output characteristics obtained for the two polarizations are shown in Fig. 7 against the absorbed pump power for two output couplers ($T_{oc}=1$ and 3%).

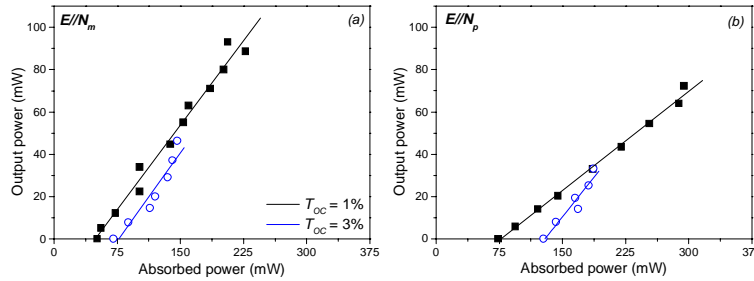


Fig. 7. Room temperature continuous-wave laser performances of Yb:KGP for $E//N_m$ (a) and $E//N_p$ (b). Solid lines are fits to the experimental points for estimation of the slope efficiency.

The relevant laser parameters (slope efficiency η with respect to the absorbed power, oscillation wavelength λ_L and threshold) are summarized in Table 3.

Table 3. Slope efficiency (η), laser wavelength (λ_L), and threshold of the $\text{KYb}_{0.024}\text{Gd}_{0.976}(\text{PO}_3)_4$ laser in dependence on the output coupler (T_{oc}) used

T_{oc} (%)	η (%)		λ_L (nm)		threshold (mW)	
	$E//N_m$	$E//N_p$	$E//N_m$	$E//N_p$	$E//N_m$	$E//N_p$
1	53.2	31.3	1017.1	1016.3	51	73.8
3	55.6	-	1013.8	1013.5	70.5	127.8
5	-	no lasing	1012.1	no lasing	131.8	no lasing

With a maximum incident pump power of roughly 2 W (corresponding to an absorbed power of 206 mW at 977.1 nm), the maximum output power for $E//N_m$ was 93 mW ($T_{oc}=1\%$). The corresponding slope efficiency was $\eta=53.2\%$. Pumping with polarization parallel to N_p , the maximum output power reached 72 mW for an absorbed power of 294 mW, also with $T_{oc}=1\%$. In this case the slope efficiency was lower, $\eta=31.3\%$. The laser thresholds for $E//N_m$ and $E//N_p$ were 51 and 74 mW, respectively, both for $T_{oc}=1\%$. The lower slope efficiency and higher threshold for $E//N_p$ can be explained by the lower gain.

For $T_{oc}=5\%$ the output power reached 12 mW (only for $E//N_m$) and reliable estimation of the slope efficiency was not possible. The oscillation wavelength was as short as 1012.1 nm in this case. The shorter wavelength at higher output coupler transmission is typical for Yb-lasers and is related to the maximum of the gain curve. In this case we have obviously oscillation on the $^2F_{5/2}(0') \rightarrow ^2F_{7/2}(2)$ transition.

Under lasing conditions the absorption of the sample was quite low (not more than 15%) but almost constant. This is a consequence of the low Yb-ion density in the crystal and the relatively low absorption cross-sections. Under non-lasing conditions the absorption was completely bleached at the maximum incident power. However, in the lasing state, the intracavity power in the three-level system of ytterbium increases the saturation intensity for the pump and this balances the bleaching effect.

5. Summary

In conclusion, we successfully grew macrodefect-free single crystals of Yb-doped KGP using the TSSG-SC technique. To the best of our knowledge, KGP crystals were doped with ytterbium for the first time. The maximum ytterbium concentration in the bulk crystal achieved until now is around $3.2 \times 10^{20} \text{ cm}^{-3}$. However, there are indications that it can be increased up to about $1 \times 10^{21} \text{ cm}^{-3}$. By measuring the dispersion of the refractive indices of KGP, we confirmed that this host possesses phase-matching properties for self-frequency doubling of the Yb-laser. We determined the Stark splitting of the two electronic states of Yb from absorption and emission measurements, both at room and low temperatures, and calculated the emission cross sections at room temperature. The upper level lifetime of Yb amounts to 1.22 ms at room temperature. Lasing has been demonstrated for the first time with $\text{KYb}_{0.024}\text{Gd}_{0.976}(\text{PO}_3)_4$. Although the maximum output power achieved (93 mW) was limited by the available size and doping level of the crystal, the more than 55% slope efficiency obtained with this first sample is rather promising for the future.

Acknowledgments

We thank C. Kränkel and K. Petermann (Hamburg University, Germany) for the measurement of the fluorescence decay time.

We acknowledge financial support from the Departament d'Universitats, Recerca i Societat de la Informació de la Generalitat de Catalunya under the Project 2005SGR658 and from MEC (Ministerio de Educación y Ciencia) of the Spanish government, under Projects MAT-05-06354-C03-02, MAT-04-20471-E and CIT-020400-2005-14. This paper is also supported by EU-Commission Project DT-CRYST (STRP-NMP3-CT-2003-505580). I.

Parreu acknowledges financial support from Fons Social Europeu i del Departament d'Universitats, Recerca i Societat de la Informació de la Generalitat de Catalunya. X. Mateos knows financial support from the Secretaria de Estado de Educación y Universidades of Spain and from the Fondo Social Europeo.